

# Quantification of memory effects in the spin-boson model

Govinda Clos\* and Heinz-Peter Breuer†

*Physikalisches Institut, Universität Freiburg, Hermann-Herder-Straße 3, D-79104 Freiburg, Germany*

(Dated: June 16, 2021)

Employing a recently proposed measure for quantum non-Markovianity, we carry out a systematic study of the size of memory effects in the spin-boson model for a large region of temperature and frequency cutoff parameters. The dynamics of the open system is described utilizing a second-order time-convolutionless master equation without the Markov or rotating wave approximations. While the dynamics is found to be strongly non-Markovian for low temperatures and cutoffs, in general, we observe a special regime favoring Markovian behavior. This effect is explained as resulting from a resonance between the system's transition frequency and the frequencies of the dominant environmental modes. We further demonstrate that the corresponding Redfield equation is capable of reproducing the characteristic features of the non-Markovian quantum behavior of the model.

## I. INTRODUCTION

Almost any realistic physical system interacts with its environment. The effects of this interaction can be described within the framework of open quantum systems [1, 2]. The coupling of a quantum system to an environment typically leads to dissipation and decoherence processes in the open system. However, it is known that due to the interaction, non-Markovian effects can emerge as well. Following the classical definition [3, 4], quantum non-Markovianity is often loosely described as the occurrence of memory effects in which the environment acts as a memory allowing the earlier open system states to have an effect on the later dynamics of the system. It is known that non-Markovian effects can play an important role in many applications [3, 5, 6], but the absence of a proper definition of non-Markovianity in the quantum case impeded systematic studies of these effects. Recently, several formal definitions for quantum non-Markovianity [7–9], which are based on different mathematical and physical concepts, have been proposed.

Here, we employ the definition developed in Ref. [7], which is based on the exchange of information between the system and its environment and enables a unique quantification of the size of quantum memory effects in the dynamics of a quantum system. We will study the behavior of this measure for a selected example: the spin-boson model, which is the paradigm of a dissipative two-level system [2, 10]. The spin-boson model has been studied extensively over the past decades and has been successfully used to describe, e.g., chemical reactions, especially charge transfer processes in the condensed phase [11], tunneling of defects and impurities in solids and metals [12], and tunneling in amorphous materials [13, 14]. Also, the famous Kondo problem [15] could be linked to the spin-boson model [16], which led to the explanation for the Kondo effect [17, 18]. Further, the dynamics of magnetic flux trapped in a SQUID ring

has also been understood with the help of this model and, based on this setup, quantum computing devices have been proposed and partially implemented [19–22]. The pursuit of the experimental realization of stable and controllable qubits has become highly important, and it is thus not surprising that quantum dots made of semiconductors have also been investigated as possible qubit implementations [23, 24]. Such quantum dots and their dissipative interaction with the surrounding components are often described by the spin-boson model. Another very promising approach to quantum computation lies in trapped ions [25], as these systems allow for a very high degree of control and long qubit lifetimes [26, 27]. Again, the spin-boson model is a key tool to a theoretical understanding of the important effects [28].

It is not only interesting to characterize memory effects in this prototypical example, but an important motivation for the present study also lies in the need for a better understanding and characterization of the properties of the non-Markovianity measure itself, especially for more complex physical systems. There are several publications studying this quantity in more detail [29], applying it to physical models [30–33], and comparing it to other measures [34–36]. Additionally, several experimental measurements of the non-Markovianity measure have been carried out recently [37, 38], demonstrating that it provides an experimentally accessible observable which quantifies memory effects. Quite recently further theoretical implications and experimental applications to nonlocal quantum memory effects have been developed [39].

The paper is organized as follows: In Sec. II we briefly present the non-Markovianity measure of Ref. [7], introduce the spin-boson model and the corresponding second-order time-convolutionless master equation, and explain the numerical simulation method used to determine the measure for quantum non-Markovianity. The numerical simulation results are discussed and linked to a theoretical interpretation in Sec. III, where we also revisit the role of the standard Markov approximation (which is not used in Sec. II). Finally, in Sec. IV we summarize our results and draw some conclusions.

---

\* govinda.clos@physik.uni-freiburg.de

† breuer@physik.uni-freiburg.de

## II. QUANTIFYING NON-MARKOVIANITY

### A. Measure for the degree of memory effects

We quantify memory effects in the dynamics of the spin-boson system, employing a recently proposed general measure for the degree of non-Markovian behavior in the evolution of an open quantum system [7]. This measure is based on the idea that Markovian time evolutions are characterized by a continuous loss of information from the open system to the environment, while non-Markovian dynamics feature a flow of information from the environment back to the open system. An appropriate tool to measure this information flow is given by the trace distance between two quantum states  $\rho_1$  and  $\rho_2$ , which is defined by [40]

$$\mathcal{D}(\rho_1, \rho_2) = \frac{1}{2} \text{Tr} |\rho_1 - \rho_2|, \quad (1)$$

where the modulus of an operator  $A$  is given by  $|A| = \sqrt{A^\dagger A}$ . The trace distance can be interpreted as the distinguishability of the states  $\rho_1$  and  $\rho_2$  [41]. We suppose that the dynamics of the open system is described by a family of trace preserving and completely positive maps  $\Phi(t)$ . Any pair of initial states  $\rho_{1,2}(0)$  then evolves into  $\rho_{1,2}(t) = \Phi(t)\rho_{1,2}(0)$  at time  $t \geq 0$ . If the family of maps  $\Phi(t)$  is divisible, e.g., if it forms a semigroup with a generator in Lindblad form [42, 43], the trace distance

$$\mathcal{D}(t) = \mathcal{D}(\rho_1(t), \rho_2(t)) = \mathcal{D}(\Phi(t)\rho_1(0), \Phi(t)\rho_2(0)) \quad (2)$$

between the time-dependent pair of states decreases monotonically [29]. This implies that the states  $\rho_1$  and  $\rho_2$  tend to become less and less distinguishable over time, which means that information about the system states is lost to the environment. On the other hand, whenever the trace distance increases, the two states become more distinguishable, and hence, information must have flowed back from the environment to the system, which is a clear signature for the presence of memory effects.

On the basis of this interpretation, the measure for the non-Markovianity of the dynamics of an open system is defined by

$$\mathcal{N}(\Phi) = \max_{\rho_{1,2}(0)} \int_{\sigma > 0} dt \sigma(t), \quad (3)$$

where  $\sigma(t) = \frac{d}{dt} \mathcal{D}(t)$  denotes the rate of change of the trace distance given by Eq. (2) and the time integration is extended over all intervals in which  $\sigma$  is positive. The measure, thus, quantifies the total backflow of information from the environment to the open system. It further involves a maximization over the initial pair of states  $\rho_{1,2}(0)$  and therefore represents a functional of the family of dynamical maps  $\Phi(t)$  describing the physical process.

By definition, the measure  $\mathcal{N}(\Phi)$  is non-negative, and we have  $\mathcal{N}(\Phi) = 0$  if and only if the process is Markovian. A nonzero measure,  $\mathcal{N}(\Phi) > 0$ , implies that the

process  $\Phi(t)$  is nondivisible and cannot be described, for example, by a time-local master equation with positive rates [29]. We note that the non-Markovianity measure  $\mathcal{N}(\Phi)$  represents a physically measurable quantity, as has been demonstrated in several recent experiments [37, 38].

### B. Spin-boson model and master equation

The spin-boson model describes a two-level system which is linearly coupled to an environment of harmonic oscillators. The Hamiltonian of the model consists of a system part  $H_S$ , an environmental part  $H_E$ , and an interaction part  $H_I$ :

$$\begin{aligned} H &= H_S + H_E + H_I \\ &= \frac{\omega_0}{2} \sigma_z + \sum_n \left( \frac{p_n^2}{2m_n} + \frac{m_n \omega_n^2}{2} x_n^2 \right) - \frac{\sigma_x}{2} \sum_n \kappa_n x_n, \end{aligned} \quad (4)$$

where  $\sigma_x$  and  $\sigma_z$  are Pauli matrices,  $\omega_0$  denotes the energy splitting of the two-level system ( $\hbar$  is set equal to 1), and  $m_n$ ,  $\omega_n$ ,  $x_n$ , and  $p_n$  represent the masses, frequencies, and position and momentum operators of the environmental oscillators, respectively. Finally,  $\kappa_n$  describes the coupling of the system to the  $n$ -th oscillator.

We assume that the system-environment coupling is weak and employ the second-order time-convolutionless master equation in the interaction picture to describe the dynamics of the open system [44–47],

$$\begin{aligned} \frac{d}{dt} \rho(t) &= -i[\tilde{H}_S(t), \rho(t)] \\ &+ \sum_{i,j=0,1} a_{ij}(t) \left( \sigma_i \rho(t) \sigma_j^\dagger - \frac{1}{2} \{ \sigma_j^\dagger \sigma_i, \rho(t) \} \right). \end{aligned} \quad (5)$$

We note that the derivation of this master equation is carried out without using the Markov or the rotating wave approximation. We have introduced the operators  $\sigma_1 = \sigma_+$  and  $\sigma_0 = \sigma_-$ . The time-dependent coefficients  $a_{ij}(t)$  form a Hermitian matrix and can be expressed in terms of the correlation functions of the environmental operator,

$$B(t) = \sum_n \frac{\kappa_n}{\sqrt{2m_n \omega_n}} (a_n e^{-i\omega_n t} + a_n^\dagger e^{i\omega_n t}), \quad (6)$$

where  $a_n^\dagger$  and  $a_n$  are the creation and annihilation operators of the environmental modes. Explicitly, we find

$$a_{11}(t) = \frac{1}{2} \int_0^t ds \text{Re} \left[ \text{Tr}_E \{ B(t) B(s) \rho_E \} e^{-i\omega_0(t-s)} \right], \quad (7)$$

$$a_{00}(t) = \frac{1}{2} \int_0^t ds \text{Re} \left[ \text{Tr}_E \{ B(t) B(s) \rho_E \} e^{+i\omega_0(t-s)} \right], \quad (8)$$

$$a_{10}(t) = \frac{1}{2} \int_0^t ds \text{Re} \left[ \text{Tr}_E \{ B(t) B(s) \rho_E \} \right] e^{-i\omega_0(t-s)}. \quad (9)$$

The time-dependent system Hamiltonian  $\tilde{H}_S(t)$  is a diagonal matrix with diagonal elements

$$h_1(t) = \frac{1}{4} \int_0^t ds \operatorname{Im} \left[ \operatorname{Tr}_E \{ B(t) B(s) \rho_E \} e^{+i\omega_0(t-s)} \right], \quad (10)$$

$$h_0(t) = \frac{1}{4} \int_0^t ds \operatorname{Im} \left[ \operatorname{Tr}_E \{ B(t) B(s) \rho_E \} e^{-i\omega_0(t-s)} \right]. \quad (11)$$

The environment is assumed to be in a thermal equilibrium state initially, i.e., we have  $\rho_E = Z^{-1} e^{-\beta H_E}$ , where  $Z$  is the partition function and  $\beta = \frac{1}{T}$  the inverse temperature (the Boltzmann constant is set equal to 1).

It is convenient to write the master equation (5) in terms of the Bloch vector  $\vec{v}(t) = \operatorname{Tr}_S \{ \vec{\sigma} \rho(t) \}$ . Transforming back to the Schrödinger picture one finds [1]

$$\frac{d}{dt} \vec{v}(t) = M(t) \vec{v}(t) + \vec{b}(t), \quad (12)$$

where

$$M(t) = \begin{pmatrix} 0 & -\omega_0 & 0 \\ \omega_0 + a_{yx}(t) & a_{zz}(t) & 0 \\ 0 & 0 & a_{zz}(t) \end{pmatrix}, \quad (13)$$

and  $\vec{b}(t) = (0, 0, b_z(t))^T$ , with real coefficients given by

$$a_{yx}(t) = -2 \operatorname{Im} \{ a_{10}(t) \} = \frac{1}{2} \int_0^t ds D_1(s) \sin \omega_0 s, \quad (14)$$

$$a_{zz}(t) = -a_{11}(t) - a_{00}(t) = -\frac{1}{2} \int_0^t ds D_1(s) \cos \omega_0 s, \quad (15)$$

$$b_z(t) = a_{11}(t) - a_{00}(t) = -\frac{1}{2} \int_0^t ds D(s) \sin \omega_0 s. \quad (16)$$

Here,  $D_1(s)$  and  $D(s)$  denote the noise and dissipation kernel of the model which can be expressed in terms of the spectral density  $J(\omega, \Omega)$  of the environmental modes as

$$D_1(s) = 2 \int_0^\infty d\omega J(\omega, \Omega) \coth \left( \frac{\omega}{2T} \right) \cos \omega s, \quad (17)$$

$$D(s) = 2 \int_0^\infty d\omega J(\omega, \Omega) \sin \omega s. \quad (18)$$

In the following we choose an Ohmic spectral density with Lorentz-Drude cutoff,

$$J(\omega, \Omega) = \frac{\gamma \omega}{\pi \omega_0} \frac{\Omega^2}{\Omega^2 + \omega^2}, \quad (19)$$

where  $\Omega$  is the cutoff frequency and  $\gamma$  defines the coupling strength.

### C. Numerical simulation

We have carried out numerical simulations to determine the non-Markovianity measure (3) for the spin-boson model. For any given pair of initial states  $\rho_{1,2}(0)$ ,

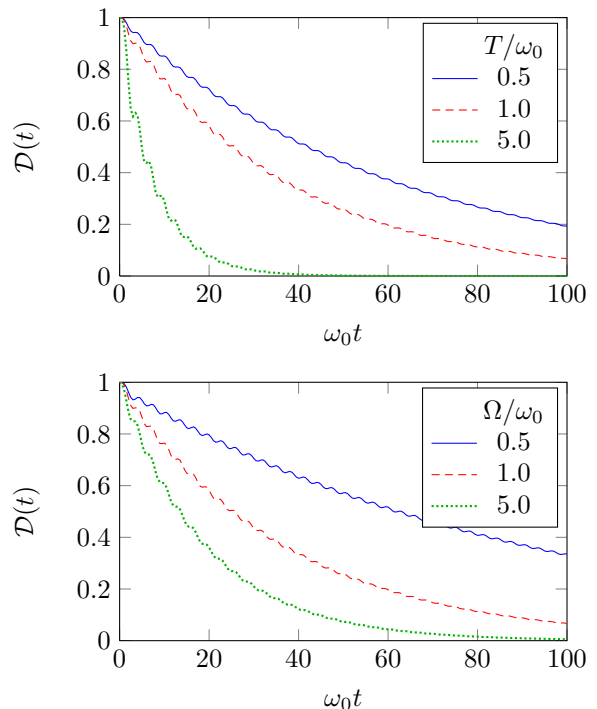


FIG. 1. (Color online) The trace distance as a function of time for various temperatures (top) and cutoffs (bottom). The parameter values of the middle curve in both plots are  $T = \omega_0$ ,  $\Omega = \omega_0$ ,  $\gamma = 0.1\omega_0$ , and  $\vec{v}_{1,2}(0) = \pm(1, 0, 0)^T$ . The other curves show the effect of a variation of *one* of these parameters.

represented by the corresponding Bloch vectors  $\vec{v}_{1,2}(0)$ , one first solves the Bloch equations (12) to determine the behavior of the trace distance by means of

$$\mathcal{D}(t) = \mathcal{D}(\rho_1(t), \rho_2(t)) = \frac{1}{2} |\vec{v}_1(t) - \vec{v}_2(t)|, \quad (20)$$

where  $|\vec{v}_1 - \vec{v}_2|$  denotes the Euclidean distance. An example is depicted in Fig. 1.

To obtain the total backflow of information given by the time integral in Eq. (3), we subdivide the time axis into sufficiently small intervals  $[t_i, t_{i+1}]$  and evaluate the quantity

$$\mathcal{N}' = \frac{1}{2} \sum_i \left[ |\vec{v}_1(t_{i+1}) - \vec{v}_2(t_{i+1})| - |\vec{v}_1(t_i) - \vec{v}_2(t_i)| \right],$$

where the sum is extended over those intervals in which the trace distance increases. The measure (3) is then found by maximizing  $\mathcal{N}'$  over all pairs of initial states. We have realized this maximization procedure numerically by a Monte Carlo sampling, drawing independent random initial state pairs from a uniform distribution over the state space.

Our goal is to study the behavior of the non-Markovianity as a function of parameters of the environment, namely, the temperature  $T$  and the cutoff fre-

quency  $\Omega$  in the spectral density. To this end, we numerically estimate the measure  $\mathcal{N}(\Phi)$  according to the above procedure for different values of these parameters. The result is a full characterization of the non-Markovian behavior in the spin-boson model depending on the properties of its environment depicted in Fig. 2. For the

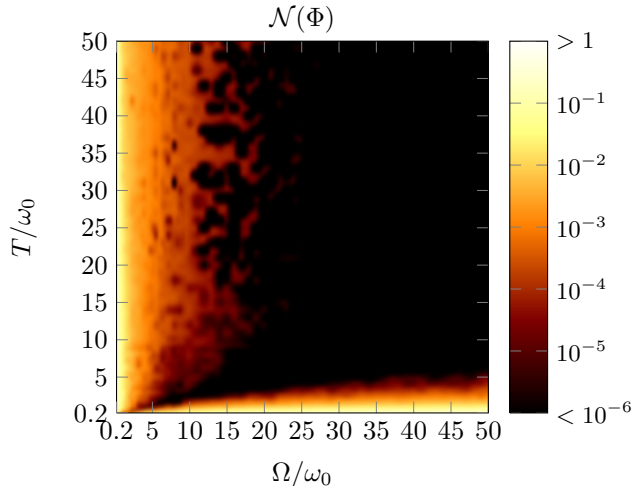


FIG. 2. (Color online) Non-Markovianity  $\mathcal{N}(\Phi)$  as a function of  $\Omega$  and  $T$  up to  $\Omega, T = 50\omega_0$ , indicated by the logarithmic colorbar.

preparation of this figure, the non-Markovianity measure has been evaluated on a grid consisting of roughly 5000 parameter combinations, with a denser sampling in the range of  $T, \Omega < 10\omega_0$  shown in Fig. 3. For each of these points, the Monte Carlo simulation to approximate the maximization over all state pairs has been done with 12000 random initial state pairs. Comparisons and tests with special fixed initial state pairs suggest that the speckled structure in Fig. 2 is due to the maximization procedure and does not mirror a physical effect. We will now discuss and interpret these results in detail.

### III. DISCUSSION AND THEORETICAL INTERPRETATION

#### A. Resonance effect

Figure 2 shows the non-Markovianity defined by Eq. (3) as a function of temperature  $T$  and environmental cutoff frequency  $\Omega$ . Note that the values of the measure  $\mathcal{N}(\Phi)$  are represented by a logarithmic colorbar for better visualization. Based on this plot, one can decide for which parameters the system behaves Markovian and for which it exhibits strong non-Markovian effects. We observe that, roughly speaking, for small cutoffs  $\Omega \lesssim \omega_0$  and for small temperatures  $T \lesssim \omega_0$  the dynamics is strongly non-Markovian, as can be seen from the high values of the measure  $\mathcal{N}(\Phi)$  in these regions. By contrast, for

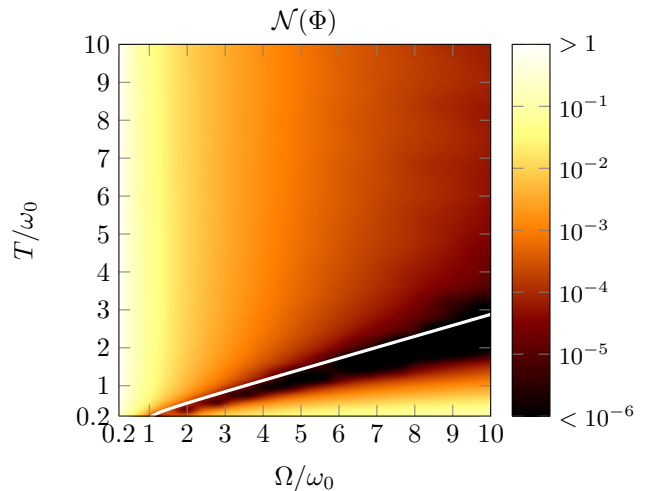


FIG. 3. (Color online) Non-Markovianity  $\mathcal{N}(\Phi)$  as a function of  $\Omega$  and  $T$  up to  $\Omega, T = 10\omega_0$ . For this range, the maximization has been refined with additional initial state pairs to yield a higher resolution. The white curve shows the parametrization of the resonance effect given by Eq. (23).

large values of both  $\Omega$  and  $T$ , the measure is zero and the dynamics is Markovian, in full agreement with the well-known quantum optical limit [1].

Our simulation results show that the non-Markovianity measure  $\mathcal{N}(\Phi)$  features a characteristic structure: It exhibits a distinct minimum, i.e., a Markovian area within a non-Markovian regime for certain values of temperature and cutoff. This can be seen more clearly in Fig. 3 which shows a magnification of the range  $\Omega, T < 10\omega_0$  obtained from a numerical simulation with higher resolution. In the following we develop a physical interpretation for this feature which obviously depends on the temperature and the cutoff frequency so that it cannot be explained by looking at the spectral density  $J(\omega, \Omega)$  only. The position of the minimum can be extracted from the Monte Carlo simulation data and the dependence is found to be nonlinear, contrary to first the impression.

The environmental modes enter the master equation via the correlation functions in Eqs. (7), (8), and (9). In particular, the coefficients  $a_{yx}(t)$  and  $a_{zz}(t)$  in the master equation depend on the noise kernel  $D_1(s)$  given in Eq. (17), which is determined by the effective spectral density

$$J_{\text{eff}}(\omega, \Omega, T) = J(\omega, \Omega) \coth\left(\frac{\omega}{2T}\right), \quad (21)$$

where  $J(\omega, \Omega)$  is defined by Eq. (19). The spectral distribution  $J_{\text{eff}}$  depends on three parameters: the environmental mode frequency  $\omega$ , the cutoff frequency  $\Omega$ , and the temperature  $T$ . One can easily see that  $J_{\text{eff}}$ , regarded as a function of  $\omega$ , has exactly one maximum at some frequency  $\omega_{\text{max}}$  and the dominant environmental modes are located around this frequency value. Under the resonance condition  $\omega_0 = \omega_{\text{max}}$  the open system sees an environmental power spectrum, which is approximately

constant around its transition frequency  $\omega_0$ , as is illustrated in Fig. 4. In the neighborhood of the transition

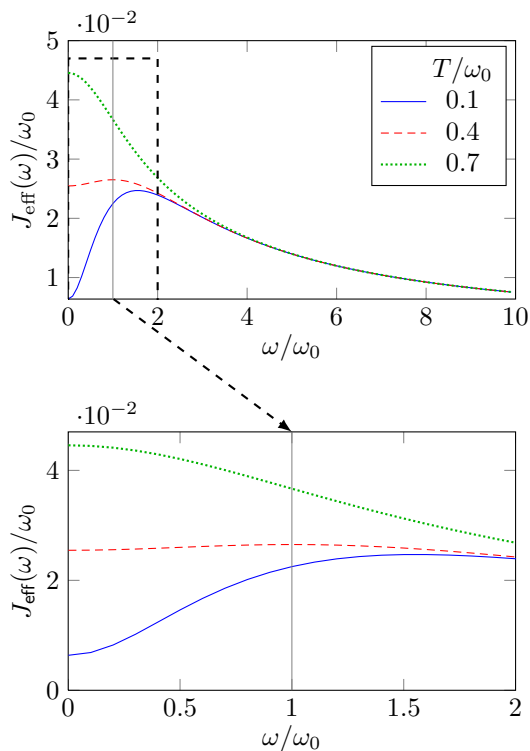


FIG. 4. (Color online) The effective spectral density  $J_{\text{eff}}(\omega)$  for a fixed cutoff  $\Omega = 1.55\omega_0$  and three different values of temperature  $T$ . The middle curve ( $T = 0.4\omega_0$ ) shows the spectral density obtained from the resonance condition (23); the other two curves correspond to detuned temperature values. The vertical line indicates the system's transition frequency  $\omega_0$ . The bottom plot shows a magnification of the top plot.

frequency of the system the spectral distribution is, thus, similar to the spectrum of white noise, and we, therefore, expect to find the region of predominantly Markovian behavior from the condition

$$\left. \frac{\partial}{\partial \omega} J_{\text{eff}}(\omega, \Omega, T) \right|_{\omega=\omega_0} = 0. \quad (22)$$

This equation defines a curve  $\Omega = \Omega_{\text{res}}(T)$  in the  $(\Omega, T)$  plane representing the points at which the system's transition frequency  $\omega_0$  is exactly in resonance with the maximum of the effective spectral density. Hence, the region of Markovian behavior should be located around this curve. To test this prediction we use Eq. (22) to obtain the following resonance condition:

$$\Omega_{\text{res}}(T) = \omega_0 \sqrt{\frac{T \sinh\left(\frac{\omega_0}{T}\right) + \omega_0}{T \sinh\left(\frac{\omega_0}{T}\right) - \omega_0}}. \quad (23)$$

This function is shown as a white curve in Fig. 3. By comparison with the dark region in the figure, representing the region of very low or even zero non-Markovianity

measure  $\mathcal{N}(\Phi)$ , we see that the resonance condition indeed explains very well the emergence of Markovian behavior embedded in a region of large non-Markovianity. We note that this picture corresponds to the results of Ref. [7], where the damped Jaynes-Cummings model, describing the interaction of a two-level system with a damped cavity mode, has been studied. For this model the non-Markovianity measure, considered as a function of the detuning between the system transition frequency and the frequency of the cavity mode, shows an analogous behavior, expressing Markovian behavior for sufficiently small detuning and a transition to non-Markovian dynamics above a certain threshold.

## B. Stationary rate approximation

The master equation (12) can be derived by employing only the Born approximation, which presupposes a weak system-environment coupling. The conventional Markov approximation consists of neglecting the time-dependence of the coefficients of the master equation  $a_{yx}(t)$ ,  $a_{zz}(t)$ , and  $b_z(t)$  and taking their asymptotic values for  $t \rightarrow \infty$  (stationary rate approximation). The resulting equation is also known as the Redfield master equation [48]. It provides an equation of motion with a time-independent generator which is not in Lindblad form and, hence, does not yield a completely positive quantum dynamical semigroup. However, for many physical problems the Redfield equation has been shown to provide a useful and accurate approximation of the reduced open system dynamics.

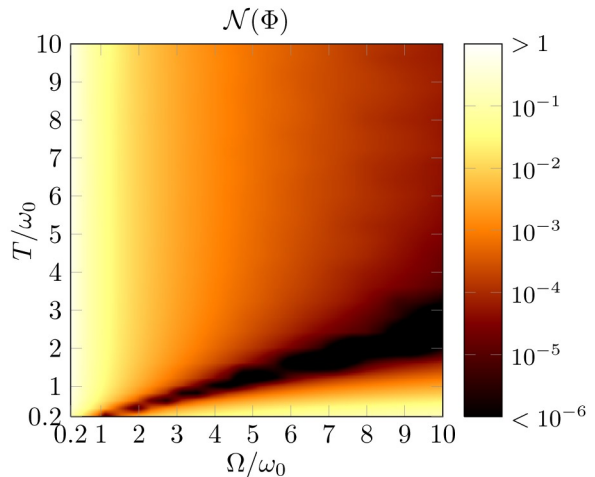


FIG. 5. (Color online) Non-Markovianity  $\mathcal{N}(\Phi)$  as a function of  $\Omega$  and  $T$  up to  $\Omega, T = 10\omega_0$  for the master equation with stationary rates (Redfield equation).

We have carried out numerical simulations to determine the non-Markovianity measure  $\mathcal{N}(\Phi)$  under the stationary rate approximation leading to the Redfield equation. Results are shown in Fig. 5. Quite remarkably,

the dynamics generated by the Redfield equation is still strongly non-Markovian in a large parameter region. Actually, comparing Figs. 5 and 3 we observe that the overall behavior of the non-Markovianity measure is qualitatively and even quantitatively very similar to the case without stationary rate approximation. Thus, we conclude that the stationary rate approximation, which is conventionally regarded as the Markov approximation, does not lead to a quantum Markov process in the sense of the definition for non-Markovianity used here.

#### IV. CONCLUSIONS

In this article we have quantified non-Markovian effects in the dynamics of the spin-boson model depending on properties of the environment. We have characterized the non-Markovianity of the dynamical map as a function of the temperature and the cutoff frequency in the spectral density. This result serves to classify different regimes in the parameter range. On the one hand, we can understand why the predictions of a Lindblad master equation fail in some applications, and, on the other hand, our findings may be used as a tool to devise experimental setups that feature especially large non-Markovian effects.

During the maximization over all initial state pairs for the evaluation of the non-Markovianity measure, we found that the main contribution to the measure stems from the time evolution of the off-diagonal elements of the system density matrix, i.e., the coherences. This fact suggests that at least in our case, the non-Markovianity is mainly a quantum effect. Consequently, a description by means of a classical rate equation might fail to reproduce important memory effects.

It is often believed that non-Markovianity is to a large extent only a transient phenomenon. However, our comparison of the results for the non-Markovianity measure applied to the full master equation with those for the master equation with stationary rate approximation (Redfield master equation) reveals that this intuition might be misleading: Although the initial oscillations of the coefficients in the master equation decay over times which are short compared to the system's relaxation time, the non-Markovianity measure steadily builds up over the whole relaxation process, showing no special significance of the transient time evolution. Consequently, this approximation yields qualitatively similar

results for the measure, despite the fact that it neglects any transient effects.

In this context, the meaning of the standard Markov approximation must be revisited. The approximation of stationary rates in the master equation is often regarded as Markovian description and the rates are called Markovian rates. However, our results demonstrate that an approximation of this kind does not necessarily lead to a Markovian dynamics in the sense of our definition in terms of the information flow. In fact, we found that the master equation with stationary rates is still capable of describing the essential features of the non-Markovian behavior. It should also be noticed in this context that in the derivation of a Lindblad master equation the rotating wave approximation is a crucial step in order to obtain a completely positive quantum dynamical semigroup. Thus, it is the combination of rotating wave and standard Markov approximation that has the desired effect of yielding a Markovian semigroup; the term *Markov approximation* can in this sense be deceptive.

The dynamics given by the master equation (12) without the rotating wave and stationary rate approximations not only shows strong non-Markovian behavior for small temperatures and/or environmental cutoff frequencies, but also features an interesting resonance effect: For a certain narrow range of parameters within the non-Markovian regime, the system exhibits Markovian dynamics. We were able to explain this effect by showing that this Markovian behavior occurs when the system transition frequency is in (or close to) resonance with the dominant modes of the environment. This can be understood by recognizing that in this case the distribution of modes in the vicinity of the system frequency resembles a uniform distribution (white noise), which clearly favors Markovian behavior. The next step towards a deeper understanding of the resonance effect is to study the behavior of the non-Markovianity measure for other models involving, in particular, structured reservoir spectral densities with several maxima or spectral gaps.

#### ACKNOWLEDGMENTS

We thank Jyrki Piilo and Elsi-Mari Laine for interesting discussions and helpful comments on the manuscript. Financial support by the German Academic Exchange Service (DAAD) is gratefully acknowledged.

---

[1] H.-P. Breuer and F. Petruccione, *The Theory of Open Quantum Systems* (Oxford University Press, Oxford, 2007).  
 [2] U. Weiss, *Quantum Dissipative Systems* (World Scientific, Singapore, 1999).  
 [3] N. G. van Kampen, *Stochastic Processes in Physics and Chemistry* (Elsevier, Amsterdam, 2007).

[4] B. Vacchini, A. Smirne, E. M. Laine, J. Piilo, and H.-P. Breuer, *New J. Phys.* **13**, 093004 (2011).  
 [5] N. G. van Kampen, *Physica* **74**, 215 (1974); *Physica* **74**, 239 (1974).  
 [6] C. W. Gardiner, *Handbook of Stochastic Methods for Physics, Chemistry and the Natural Sciences* (Springer, Berlin, 2004).

- [7] H.-P. Breuer, E.-M. Laine, and J. Piilo, Phys. Rev. Lett. **103**, 210401 (2009).
- [8] A. Rivas, S. F. Huelga, and M. B. Plenio, Phys. Rev. Lett. **105**, 050403 (2010).
- [9] M. M. Wolf, J. Eisert, T. S. Cubitt, and J. I. Cirac, Phys. Rev. Lett. **101**, 150402 (2008).
- [10] A. J. Leggett, S. Chakravarty, A. T. Dorsey, M. P. A. Fisher, A. Garg, and W. Zwerger, Rev. Mod. Phys. **59**, 1 (1987).
- [11] A. Garg, J. N. Onuchic, and V. Ambegokar, J. Chem. Phys. **83**, 4491 (1985).
- [12] B. Golding, N. M. Zimmerman, and S. N. Coppersmith, Phys. Rev. Lett. **68**, 998 (1992).
- [13] J. Stockburger, M. Grifoni, M. Sassetti, and U. Weiss, Z. Phys. B **94**, 447 (1994).
- [14] A. Würger, Phys. Rev. B **57**, 347 (1998).
- [15] J. Kondo, Prog. Theor. Phys. **32**, 37 (1964).
- [16] S. Chakravarty, Phys. Rev. Lett. **49**, 681 (1982).
- [17] J. Kondo, Physica B+C **125**, 279 (1984).
- [18] J. Kondo, *Two-Level Systems in Metals*, in Fermi Surface Effects, Springer Series in Solid-State Physics, Vol. 77 (Springer, Berlin, 1988).
- [19] Y. Nakamura, Y. A. Pashkin, and J. S. Tsai, Nature **398**, 786 (1999).
- [20] I. Chiorescu, Y. Nakamura, C. J. P. M. Harmans, and J. E. Mooij, Science **299**, 1869 (2003).
- [21] Y. Makhlin, G. Schön, and A. Shnirman, Rev. Mod. Phys. **73**, 357 (2001).
- [22] D. Vion, A. Aassime, A. Cottet, P. Joyez, H. Pothier, C. Urbina, D. Esteve, and M. H. Devoret, Science **296**, 886 (2002).
- [23] T. Hayashi, T. Fujisawa, H. D. Cheong, Y. H. Jeong, and Y. Hirayama, Phys. Rev. Lett. **91**, 226804 (2003).
- [24] J. R. Petta, A. C. Johnson, C. M. Marcus, M. P. Hanson, and A. C. Gossard, Phys. Rev. Lett. **93**, 186802 (2004).
- [25] J. I. Cirac and P. Zoller, Phys. Rev. Lett. **74**, 4091 (1995).
- [26] D. J. Wineland and D. Leibfried, Laser Phys. Lett. **8**, 175 (2011).
- [27] H. Häffner, C. F. Roos, and R. Blatt, Phys. Rep. **469**, 155 (2008).
- [28] D. Porras, F. Marquardt, J. von Delft, and J. I. Cirac, Phys. Rev. A **78**, 010101(R) (2008).
- [29] E.-M. Laine, J. Piilo, and H.-P. Breuer, Phys. Rev. A **81**, 062115 (2010).
- [30] T. J. G. Apollaro, C. Di Franco, F. Plastina, and M. Paternostro, Phys. Rev. A **83**, 032103 (2011).
- [31] L. Mazzola, E. M. Laine, H.-P. Breuer, S. Maniscalco, and J. Piilo, Phys. Rev. A **81**, 062120 (2010).
- [32] P. Rebentrost and A. Aspuru-Guzik, J. Chem. Phys. **134**, 101103 (2011).
- [33] P. Haikka, S. McEndoo, G. De Chiara, G. M. Palma, and S. Maniscalco, Phys. Rev. A **84**, 031602 (2011).
- [34] D. Chruściński, A. Kossakowski, and A. Rivas, Phys. Rev. A **83**, 052128 (2011).
- [35] P. Haikka, J. D. Cresser, and S. Maniscalco, Phys. Rev. A **83**, 012112 (2011).
- [36] H.-S. Zeng, N. Tang, Y.-P. Zheng, and T.-T. Xu, arXiv:1205.6020v1[quant-ph].
- [37] B.-H. Liu, L. Li, Y.-F. Huang, C.-F. Li, G.-C. Guo, E.-M. Laine, H.-P. Breuer, and J. Piilo, Nature Phys. **7**, 931 (2011).
- [38] J.-S. Tang, C.-F. Li, Y.-L. Li, X.-B. Zou, G.-C. Guo, H.-P. Breuer, E.-M. Laine, and J. Piilo, EPL **97**, 10002 (2012).
- [39] E.-M. Laine, H.-P. Breuer, J. Piilo, C.-F. Li, G.-C. Guo, Phys. Rev. Lett. **108**, 210402 (2012).
- [40] M. A. Nielsen and I. L. Chuang, *Quantum Computation and Quantum Information* (Cambridge University Press, Cambridge, 2000).
- [41] M. Hayashi, *Quantum Information* (Springer, Berlin, 2006).
- [42] G. Lindblad, Comm. Math. Phys. **48**, 119 (1976).
- [43] V. Gorini, A. Kossakowski, and E. C. G. Sudarshan, J. Math. Phys. **17**, 821 (1976).
- [44] F. Shibata, Y. Takahashi, and N. Hashitsume, J. Stat. Phys. **17**, 171 (1977).
- [45] N. Hashitsume, F. Shibata, and M. Shingu, J. Stat. Phys. **17**, 155 (1977).
- [46] F. Shibata, Y. Takahashi, and N. Hashitsume, J. Stat. Phys. **17**, 171 (1977); S. Chaturvedi and F. Shibata, Z. Phys. B **35**, 297 (1979).
- [47] M. Tokuyama and H. Mori, Prog. Theor. Phys. **55**, 411 (1976).
- [48] A. G. Redfield, IBM J. Res. Dev. **1**, 19 (1957).